UNIVERSIDADE DO VALE DO RIO DOS SINOS - UNISINOS
UNIDADE ACADÊMICA DE PESQUISA E PÓS-GRADUAÇÃO
PROGRAMA DE PÓS-GRADUAÇÃO EM GEOLOGIA
NÍVEL MESTRADO

EMANUEL MENDONÇA FRANCISCO

MUDANÇAS HIDROCLIMÁTICAS E NO PADRÃO DE OXIGENAÇÃO DE ÁGUA DE FUNDO AO LONGO DO LIMITE TRIÁSSICO-JURÁSSICO NA SEÇÃO LEVANTO-MAINO, PERU: POSSÍVEIS GATILHOS VULCÂNICOS

São Leopoldo
2022

EMANUEL MENDONÇA FRANCISCO

HYDROCLIMATE AND DEEP WATER OXYGENATION CHANGES ACROSS THE TRIASSIC-JURASSIC BOUNDARY AT THE LEVANTO-MAINO SECTION, PERU: POSSIBLE VOLCANIC TRIGGERS

Artigo apresentado como requisito parcial para obtenção do título de Mestre em Geologia, pelo Programa de Pós-Graduação em Geologia da Universidade do Vale do Rio dos Sinos - UNISINOS

Orientador: Prof. Dr. Karlos Guilherme Diemer Kochhann

São Leopoldo

2022

F819m Francisco, Emanuel Mendonça.

Mudanças hidroclimáticas e no padrão de oxigenação de água de fundo ao longo do limite Triássico-Jurássico na seção Levanto-Maino, Peru : possíveis gatilhos vulcânicos / Emanuel Mendonça Francisco. – 2022.

42 f. : il. ; 30 cm.

Artigo (mestrado) – Universidade do Vale do Rio dos Sinos, Programa de Pós-Graduação em Geologia, 2022.

"Orientador: Prof. Dr. Karlos Guilherme Diemer Kochhann."

Dados Internacionais de Catalogação na Publicação (CIP)
(Bibliotecária: Amanda Schuster – CRB 10/2517)

AGRADECIMENTOS

Os autores agradecem à empresa Nova Analytic por gentilmente conceder o Direct Mercury Analyzer (DMA-80 evo) para uso em nosso laboratório. Agradecer à Fundação Coordenação de Aperfeiçoamento de Pessoal de Nível Superior (CAPES) pela bolsa e agradecer pelo crescimento da ciência. Agradecer também à ITT OCEANEON por ter uma estrutura que nos permitiu realizar todas as amostras em um só lugar. Aos professores Gerson Fauth e Farid Chemale Jr pelo fornecimento das amostras para o estudo. Aos colegas do Laboratório Itt, Marlone Bonn e Valeska Meirelles pela realização das amostras, ao Prof Karlos Kochhann pela correção da tradução do artigo. Ao serviço geológico peruano, em especial a Elvis Chimpay, que nos conduziu até os afloramentos. Gostaria de agradecer ao Programa de Pós-Graduação em Geologia (Ppgeo) da Unisinos por todas as discussões que fizeram este trabalho avançar, e a todos que contribuíram para que este artigo fosse escrito, seja por meio de conversas no corredor ou discussões científicas sobre o artigo.

A minha familia que desde cedo sempre me apoiou nesta caminhada, expecialmente a minha mãe, Maria Bumba pela força e o incentivo, o meu muito obrigado! A minha namorada Roberta dos Santos, que me incentivou nestes dois anos a dar o meu melhor todos os dias, embora havia dias que pareciam que não ter fim, o meu muito obrigado, te amo.

Ao meu orientador Karlos Kochhann, foram 3 anos se for pensar desde o TCC, o meu muito obrigado por teres me puxado e incentivado, havia horas que pensava que a dissertação não sairia, mas o teu incentivo e simplicidade em lidar com a pesquisa me fizeram continuar, meu muito obrigado.

A monografia não basta ser boa, tem
Parecer boa. “Autor desconhecido”

LIST OF FIGURES

SUMMARY

RESUMO

A evolução da Terra é marcada por diferentes períodos de extinção em massa, sendo as cinco principais chamadas de Big Five. Muitas vezes estas extinções estão associadas as Grandes Províncias Ígneas (Large Igneous province – LIPs). A transição Triássico-Jurássico (Triassic-Jurassic boundary - TJB) apresenta uma dessas extinções, cujas características são típicas de eventos hipertermais. Essa extinção foi associada com a LIP da Província Magmática do Atlântico Central (Central Atlantic magmatic province – CAMP) cujas consequências incluem anoxia, mudança climática e crises de biocalcificação. O entendimento destas questões são fatores cruciais, uma vez que se está a viver atualmente uma nova e possível extinção em massa onde o homem é o principal agente de mudança climática. O entendimento do comportamento dos ecossistemas passados e seu tempo de recuperação nos ajudarão a entender e prever impactos futuros das atividades antropogênicas. A vasta concentração de pesquisas nas bacias Europeias e Norte Americanas permitem um entendimento maior para esta transição naquelas localidades, sendo que os registros fora destas ainda são escassos. Aqui nós trazemos uma abordagem multiproxie que correlaciona mudanças climáticas, condições de oxigenação e possíveis registros distais do vulcanismo CAMP no evento de extinção do final do Triássico (End Triassic Extinction- ETE) e no TJB. Os registros intempéricos e climáticos indicam uma mudança das condições hidroclimáticas que iniciam com a excursão negativa dos isótopos de Carbono (carbon Isotopic Excursion -CIE) que precede o TJB. As águas de fundo permaneceram óxicas a disóxicas durante o TJB, conforme evidenciado pelos proxies redox, contrastando com padrões descritos em sessões marinhas rasas. As concentrações elevadas de Hg e Hg/TOC ocorreram durante a CIE negativa, o que sugere o registro da atividade Vulcânica do CAMP para a sessão Levanto-Maino, no Peru. De modo geral, nosso estudo evidencia a importância da seção Levanto-Maino para compreender as condições ambientais marinhas profundas associadas ao ETE e ao TJB.

Keywords: Extinção do final do Triássico (ETE), Província Magmática do Atlântico Central (CAMP), concentrações de mercúrio, Levanto Peru.

APRESENTAÇÃO

A transição entre os períodos Triássico e Jurássico é marcado por uma das grandes extinções na história do planeta, onde cerca de 73% da biodiversidade foi perdida, tanto nos oceanos quanto nos continentes (Sepkoski, 1996). As causas e consequências desta extinção têm sido estudadas por tempos e atribuídas a duas linhas de raciocínio: uma que defende o impacto de bólidos (Olsen, 2002) e outra que é associada ao vulcanismo da Província Magmática do Atlântico Central (CAMP) (Marzoli et al., 2004; Pálfy et al., 2001). Afloramentos da seção típica desta transição têm sido estudadas em Queen Charlotte Islands (Ward et al., 2001), Csovar na Hungria (Kovács et al., 2020; Pálfy et al., 2001), sucessões em Nevada (Blackburn et al., 2013; Guex et al., 2004), Peru (Guex et al., 2012; Hillebrandt, 1994; Schaltegger et al., 2008; Wotzlaw et al., 2014; Yager et al., 2021, 2017), Àustria (Hillebrandt et al., 2013; Lindström et al., 2017a), Stenlille na Dinamarca (Lindström et al., 2017a), e em St. Audrie's Bay na Inglaterra (Hesselbo et al., 2020, 2002; Whiteside et al., 2007). Esses estudos focaram principalmente em compreender a transição entre os dois períodos, os efeitos da extinção e as consequências do Vulcanismo da LIP (*Large Igneous Province - LIP)*. Consequências da colocação da CAMP incluem a liberação de gases de efeito estufa na atmosfera e nos oceanos, que elevou os níveis atmosféricos de CO_2 levando ao efeito estufa e à intensificação do ciclo hidrológico (McElwain et al., 1999; Schaller et al., 2012). A alta pCO_2 atmosférica pode ter levado à acidificação dos oceanos (Greene et al., 2012; Hautmann et al., 2008), agindo como um mecanismo de extinção no ambiente marinho.

Quase todos os afloramentos estudados se situam no hemisfério norte, sendo a Bacia de Pucará, no Peru uma das poucas do hemisfério sul. A Formação Aramachay (Grupo Pucará) apresenta um dos melhores registros sedimentares abrangendo o TJB no mundo, onde afloram várias faixas das unidades do Triássico e o contato com o Jurássico (Hillerbrandt, 1994). Estudos recentes na seção entre as localidades de Levanto e Maino, com novas datações de camadas de tufos vulcânicos (Schaltegger et al., 2008; Schoene et al., 2010), e registros de isótopos estáveis de carbono (Yager et al., 2017), permitiram que a bacia fosse correlacionada com outras bacias que registram o TJB. Um novo *proxy* de anomalia de mercúrio (concentrações de Hg e razão Hg/TOC) tem sido utilizado para rastrear o vulcanismo das LIPs (Grasby et al., 2019; Percival et al., 2017; Thibodeau et al., 2016; Yager et al., 2021), e o seu

uso para o entendimento do TJB na seção Levanto-Maino é promissor para a compreensão das possíveis consequências do vulcanismo LIP.

Para expandir o conhecimento sobre esta seção e a possível correlação com o magmatismo CAMP, este trabalho teve como objetivo realizar uma análise paleoclimática e paleoceanográfica. Foram utilizados proxies geoquímicos para aporte sedimentar, mudança climática, condições de oxigenação de massas de água de fundo e preservação de carbonato e carbono orgânico. Influências do vulcanismo foram interpretadas a partir das anomalias de mercúrio e tentou-se inferir quais as suas implicações para a transição entre o Triássico e o Jurássico.

Hipótese: Durante o trabalho de conclusão de curso (TCC) foi observada na seção Levanto-Maino, uma mudança na paleoprodutividade e aumento do aporte sedimentar terrígeno na passagem Triassico-Jurássico. Este colapso brusco de paleoprodutividade foi observado por Ward et al., (2001) em Queen Charlotte Islands (British Columbia, Canadá), que estudou a extinção dos radiolários e o desaparecimento dos bivalves *Monotis* no limite T-J. Essas mudanças paleoambientais ocorriam próximas aos níveis de cinza vulcânica, sugerindo uma possível relação com o CAMP.

A partir destas hipóteses foi desenvolvido um estudo que nos permitiu concluir que:

- O possível colapso da produtividade primária no TJB é correlacionado com uma CIE negativa, e caracterizado por uma queda nos teores de carbono orgânico total (COT) dos sedimentos.
- Uma mudança no hidrolima local, para condições mais úmidas, ocorreu na passagem Triássico-Jurássico.

Essas mudanças paleoambientais são correlacionáveis as primeiras intrusões do CAMP datadas

O presente foi desenvolvido desde o (TCC - 2019). Proxies paleoclimáticos foram medidos durante as atividades do TCC e indicadores das condições de oxigenação das águas de fundo e de atividade vulcânica foram medidos durante as

atividades de mestrado. O artigo foi submetido ao periódico Paleogeography, Palaeoclimatology, Palaoecology, conceito Qualis-CAPES A2.

Comprovante de submissão:

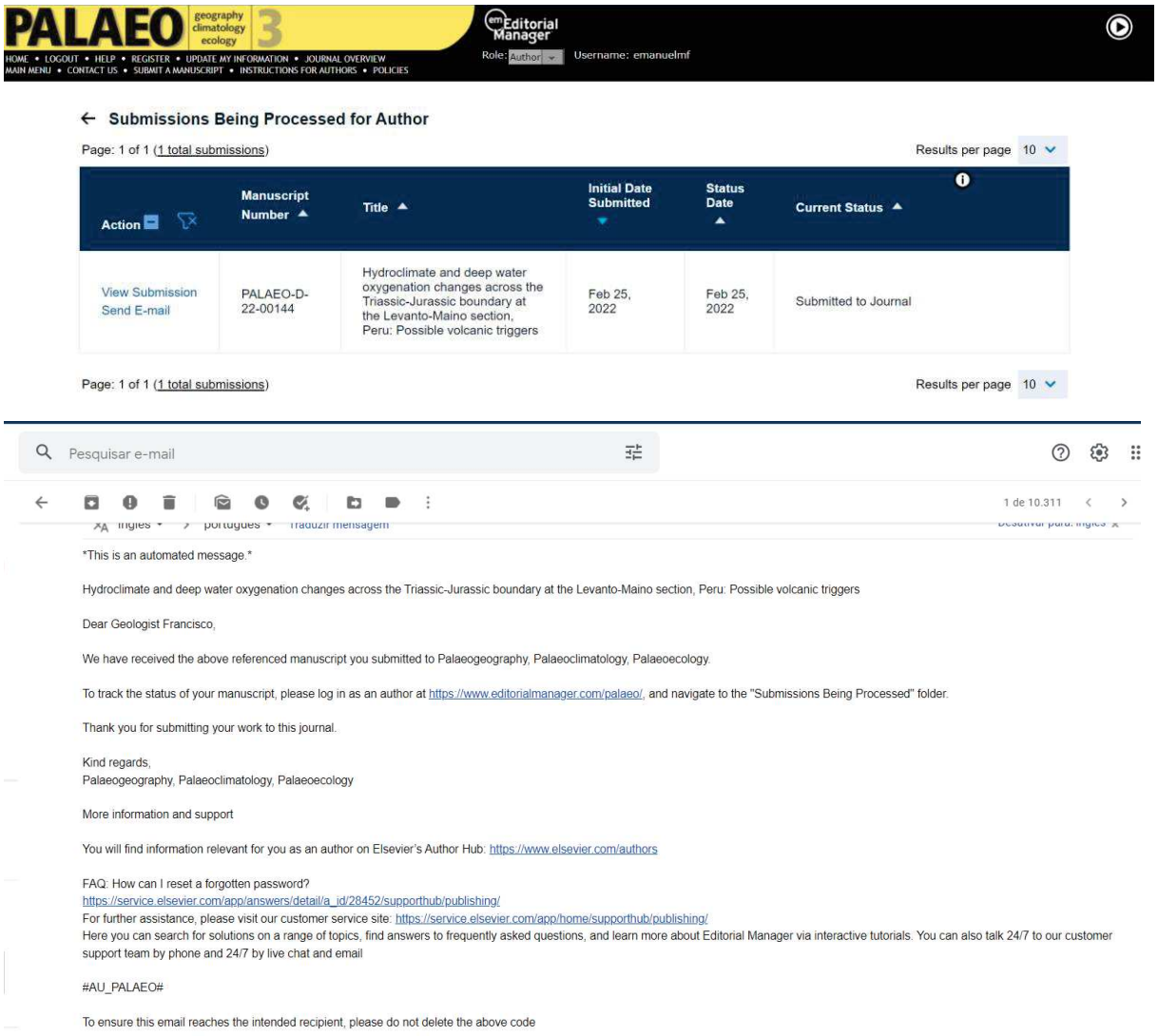

PALAEO geography climatology ecology 3

HOME • LOGOUT • HELP • REGISTER • UPDATE MY INFORMATION • JOURNAL OVERVIEW
MAIN MENU • CONTACT US • SUBMIT A MANUSCRIPT • INSTRUCTIONS FOR AUTHORS • POLICIES

Editorial Manager

Role: Author Username: emanuelmf

← Submissions Being Processed for Author

Page: 1 of 1 (1 total submissions) Results per page 10

Action	Manuscript Number	Title	Initial Date Submitted	Status Date	Current Status
View Submission Send E-mail	PALAEO-D-22-00144	Hydroclimate and deep water oxygenation changes across the Triassic-Jurassic boundary at the Levanto-Maino section, Peru: Possible volcanic triggers	Feb 25, 2022	Feb 25, 2022	Submitted to Journal

Page: 1 of 1 (1 total submissions) Results per page 10

Pesquisar e-mail

1 de 10.311

This is an automated message.

Hydroclimate and deep water oxygenation changes across the Triassic-Jurassic boundary at the Levanto-Maino section, Peru: Possible volcanic triggers

Dear Geologist Francisco,

We have received the above referenced manuscript you submitted to Palaeogeography, Palaeoclimatology, Palaeoecology.

To track the status of your manuscript, please log in as an author at https://www.editorialmanager.com/palaeo/, and navigate to the "Submissions Being Processed" folder.

Thank you for submitting your work to this journal.

Kind regards,
Palaeogeography, Palaeoclimatology, Palaeoecology

More information and support

You will find information relevant for you as an author on Elsevier's Author Hub: https://www.elsevier.com/authors

FAQ: How can I reset a forgotten password?
https://service.elsevier.com/app/answers/detail/a_id/28452/supporthub/publishing/
For further assistance, please visit our customer service site: https://service.elsevier.com/app/home/supporthub/publishing/
Here you can search for solutions on a range of topics, find answers to frequently asked questions, and learn more about Editorial Manager via interactive tutorials. You can also talk 24/7 to our customer support team by phone and 24/7 by live chat and email

#AU_PALAEO#

To ensure this email reaches the intended recipient, please do not delete the above code

MANUSCRITO

Hydroclimate and deep water oxygenation changes across the Triassic-Jurassic boundary at the Levanto-Maino section, Peru: Possible volcanic triggers

Emanuel Mendonça Francisco[*,a], Karlos Guilherme Diemer Kochhann[a,b], Gerson Fauth[a,b], Farid Chemale Jr.[a], Luiza Carine Silva[b], Elvis Sanchez Chimpay[c], Valeska Meirelles[b]

[a] Programa de Pós-graduação em Geologia, Universidade do Vale do Rio dos Sinos, 93022-220, São Leopoldo, RS, Brazil
[b] Instituto Tecnológico de Paleoceanografia e Mudanças Climáticas – Itt Oceaneon- Universidade do Vale do Rio dos Sinos, São Leopoldo, RS, Brazil
[c] Instituto Geológico, Minero y Metaturgico - INGEMMET, Lima, Peru

Abstract: The Triassic-Jurassic transition records one of the main mass extinctions of the Phanerozoic, which appears to be linked to environmental changes caused by volcanism of the Central Atlantic Magmatic Province (CAMP). Evidence of anoxia, climate change, and a biocalcification crisis are described as effects of the release of volcanic greenhouse gases. However, paleoenvironmental proxies for deep marine sections spanning the Triassic-Jurassic boundary (TJB) are scarce outside Europe and North America. We present geochemical proxies for Peru's Levanto-Maino section, which presents a complete record across the TJB interval. Log(K/Fe) records depict a shift from drier to wetter hydroclimate conditions, correlated with the onset of the negative carbon isotope excursion (CIE) that preceded the TJB. This interval was also characterized by oxic to dysoxic bottom waters, as evidenced by the U/Mo, V/(V+Ni), Ni/Co and V/Cr ratios, within the End Triassic Extinction (ETE) interval of the latest Triassic. Mercury concentrations and the Hg/TOC ratio also increase within negative

[*] corresponding author. Emanuel Mendonça Francisco.
E-mail adress: emanuelmf.francico@gmail.com

CIE, suggesting that the Levanto-Maino section also presents a distal (indirect) record of CAMP activity. From the negative CIE toward the TJB, bottom water oxygenation improved in opposition to the patterns described for shallower marine sections. In summary, the Levanto-Maino section can improve our understanding of the ETE and TJB in a deep marine setting.

Keywords, Late Triassic extinction (ETE); Central Atlantic Magmatic Province (CAMP); Hg concentration; Levanto-Maino Peru.

1 INTRODUCTION

Earth's history is marked by several periods of increased speciation and extinction rates. Five major episodes of mass extinctions, called the “big five” (Raup and Sepkoski, 1982), occurred during the Phanerozoic and were characterized by expressive biodiversity declines. The Triassic-Jurassic transition records one of these mass extinctions, when approximately 40 to 73% of biodiversity was lost (Alroy, 2010; Sepkoski, 1996). This transition was synchronous with the emplacement of a Large Igneous Province (LIPs), the Central Atlantic Magmatic Province (CAMP), whose volcanism and release of greenhouse gases and toxic compounds has been interpreted as the trigger for the observed environmental and climatic changes across the Triassic-Jurassic boundary (TJB; Marzoli et al., 2004, 1999; Van De Schootbrugge et al., 2009). The release of these gases into the atmosphere and oceans raised pCO_2 levels, leading to greenhouse conditions and intensification of the hydrological cycle (McElwain et al., 1999; Schaller et al., 2012). Stomatal index data from plant leaves suggested establishment of a super greenhouse climate state,

when atmospheric CO_2 concentrations hovered at around 2000 ppm and global mean temperatures increased by 3 to 4 °C (McElwain et al., 1999). These high atmospheric pCO_2 may have led to ocean acidification (Greene et al., 2012; Hautmann et al., 2008), acting as an extinction mechanism in marine environments.

This perturbation of the carbon cycle is recorded as multiple stable carbon isotope excursions (CIEs) in different basins around the world (Hesselbo et al., 2002; Lindström et al., 2017a; Pálfy et al., 2001; Van De Schootbrugge et al., 2008; Yager et al., 2017). These excursions indicate sudden injections of huge amounts of ^{13}C-depleted CO_2 into the ocean-atmosphere system (Marzoli et al., 2018), although its origin (e.g., dissociation of hydrates from the ocean floor, thermogenic production of methane from sediments, volcanic CO_2 release) is still debated (Bachan and Payne, 2016; Hesselbo et al., 2002; Marzoli et al., 2017; Paris et al., 2010; Ruhl et al., 2011). Several questions are still debated regarding whether volcanism played a key role in extinction (Whiteside et al., 2007). Alternative scenarios propose an extraterrestrial impact similar to K-Pg (Olsen, 2002), and rapid changes of sea level with widespread anoxia (Hallam, 1995; Hallam and Wignall, 1999).

There is a lack of knowledge of paleoenvironmental conditions of deep marine settings across the TJB, since most of faunal data used to assess ecological recovery is described from shallow marine sections (Thibodeau et al., 2016). Additionally, there are only few studies of sections outside Europe and North America, making it difficult to constrain a TJB scenario in other Panthalassa regions. Here we present a multiproxy study of the Levanto-Maino section in Peru, a complete deep marine record of the TJB, spanning the late Rhaetian to the early Sinemurian (Von Hillebrandt, 2000). Our study allows us to reconstruct hydroclimate conditions, sedimentary input, and bottom water oxygenation across the TJB. We also compare

paleoenvironmental proxies with Hg-based volcanic activity tracers to establish possible links between CAMP volcanic activity and environmental reorganizations across the TJB.

2 GEOLOGICAL SETTINGS

The Utcubamba Valley in Peru is one of the best locations worldwide where upper Triassic (Raethian) to lower Jurassic (Hettangian) strata crop out, with abundant occurrences of fossils such as ammonites (Hillenbradt, 1994). The sedimentary basins in Peru present remarkable structural control, mainly related to Neoproterozoic and Middle Proterozoic lineaments, consisting of NNE and NW structures, respectively (Tankard, 2002). The study area is located in the Pucará Basin, whose sedimentary record ranges from the Devonian to the Cretaceous, with deposition predominantly in the NNW direction, extending from northern Peru to the central part of the country (Rosas et al., 2007). The basin underwent a subsidence process induced by basement faults, which was followed by a phase of tension relaxation that caused generalized subsidence with establishment of a broad epicontinental sea (Rosas et al., 2007).

The Pucará Group ranges in age from the upper Triassic to the middle Jurassic, and consists of sandstones, claystones, and limestones (Rosas et al., 2007). It is divided into the Chambará, Aramachay and Condorsinga formations (fig.1). The fossil-rich Aramachay Formation, the focus of this work, is characterized by bituminous shales, sandstones, carbonates, cherts, and phosphate concretions (Hillebrandt, 1994), containing tuffs in the upper section (Rosas et al., 2007). According to Rosas et al. (2007), it records the deepening of a carbonate platform in

a dominantly anoxic environment, ranging in age from Raethian to Sinemurian, and adjacent to a volcanic arc that was active between the late Triassic (Norian) to early Jurassic (Schaltegger et al., 2008). Schaltegger et al. (2008) classified the stratigraphic ranges of ammonite in the Levanto section, which allow correlation with other basins.

The section studied in our work is located between the localities of Levanto and Maino (fig.1) and has well-constrained ammonite biostratigraphy (Schaltegger et al., 2008), as well as of dated ash layers (Guex et al., 2012; Schoene et al., 2010; Wotzlaw et al., 2014). Field observations demonstrate a relatively uniform section, composed of thin to thick layers of carbonates and claystones, with some carbonate concretions at the session's top. The lower part of the section (0-62m) is stratified with centimetric to millimetric ash layers. From 62 to 105 m ash layers are often occurring, and sediment beds become thicker. Petrographic data from Yager et al. (2017) confirmed no sudden variation in lithology throughout the Levanto-Maino Section.

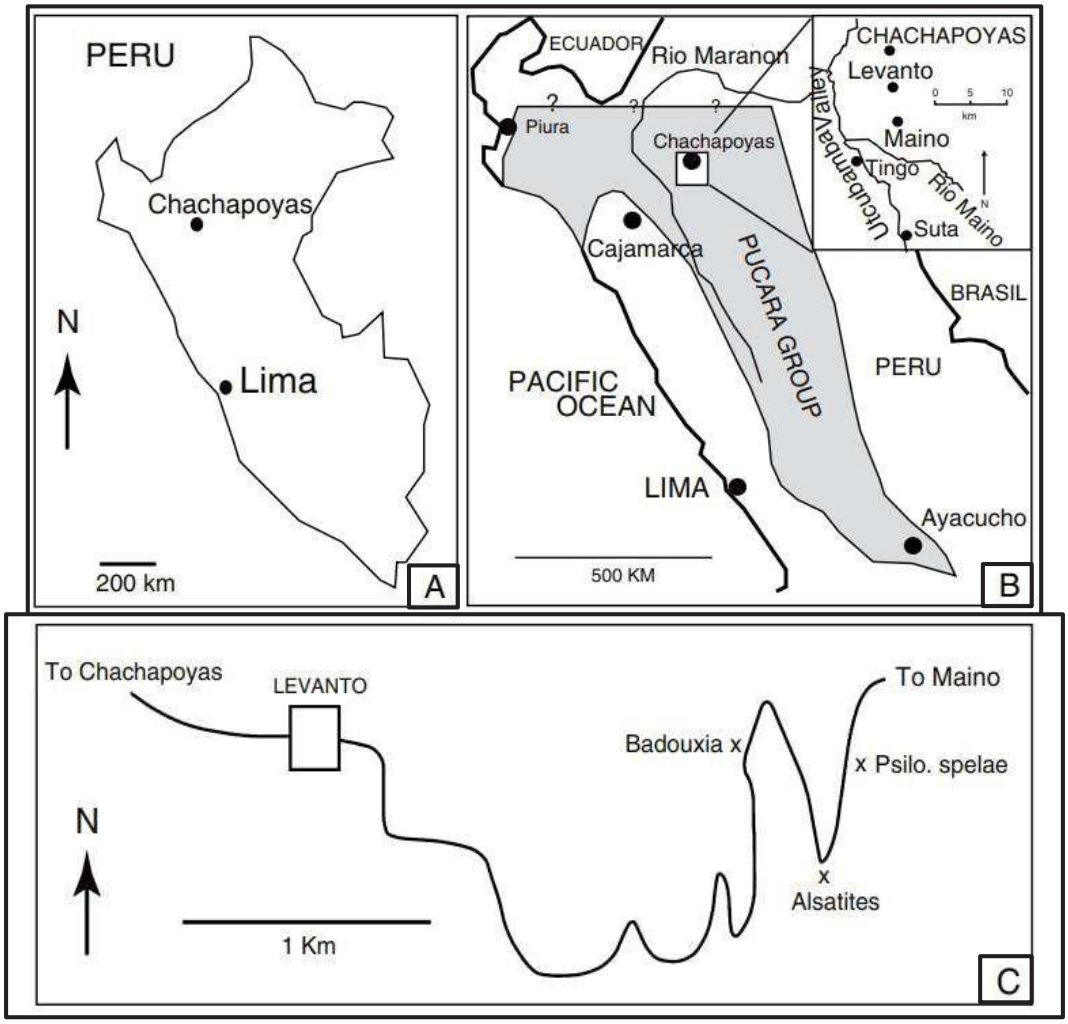

Fig. 1 - Location of the studied section and detailed map of the Levanto–Maino road with the location of some marker ammonites (modified from Guex et al., 2012)

3 MATERIAL AND METHODS

3.1 Section location and sampling strategy

We collected 124 samples within a 97.5 m-long section between the cities of Levanto and Maino (Fig. 1; 06°18'15,1"S, 77°53'03,7"W). The studied sedimentary succession is dominantly composed of limestone, interbedded with shale levels. Sampling was performed every 50 cm up to a height of 54 m in the profile, and higher

than that samples were collected every 30 cm because of the proximity to the TJB. Highly weathered samples were avoided, and only fresh rocks were collected.

3.2 Carbonate and organic carbon contents

For the determination of total carbon (TC), sediment aliquots of 0.26 g were measured on a LECO SC-144DR carbon and sulfur analyzer by combustion at temperatures between 1300 °C and 1350 ºC. For total organic carbon (TOC) analyses, sediment aliquots of 0.26 g were acidified with HCl, and, afterward, washed with deionized water heated to 100 ºC until neutral pH was achieved (repeated about eight times). After drying at 40 ºC, samples were measured as with TC analyses. Carbonate ($CaCO_3$) content was estimated based on TOC and TC measurements according to the equation: $CaCO_3$ (%) = (TC – TOC) * 8.33 (Stax and Stein, 1995). All analyses were performed at the Technological Institute for Paleoceanography and Climate Change (itt Oceaneon; UNISINOS University).

3.3 Sediment elemental ratios

For elemental analysis, an Epsilon 1 X-ray fluorescence spectrometer (Panalytacal) was used. Samples were initially fragmented in an agate mortar, and ~5 g sample aliquots were dried in an oven at 40 ºC for 2 hours. Elemental analyzes are reported as raw intensities (cps; counts per second) and the values were later interpreted in the form of elemental logarithmic ratios. Measured element intensities depend on the element concentration, but also on matrix effects, physical properties, and sample geometry (Weltje and Tjallingii, 2008). To minimize these effects, logarithmic ratios or normal ratios of two elements are used, which can be interpreted directly as the relative concentration of the concentration of these elements (Tjallingii

et al., 2010; Weltje and Tjallingii, 2008). The specific filter types, voltages and amperages used in the analyzes are summarized in Supplementary Table S1. All analyses were performed at itt OCEANEON (UNISINOS University). Log(K/Fe) was used to characterize weathering intensity throughout the section (Croudace and Rothwell, 2015; Jaeschke et al., 2007; Kwiecien et al., 2009).

3.4 Mercury analyses

Mercury (Hg) measurements were run with a direct mercury measuring device, model DMA-80 *evo* tricell double bean (Millestone). Sediment aliquots of 0.03 g were analyzed without any pre-treatment. Accuracy of Hg measurements was checked by measuring the certified reference material (CRM) NIST 1646a, as reported in Supplementary Table S2. All analyses were performed at itt OCEANEON (UNISINOS University).

3.5 Redox proxies

Sample preparation for analysis of redox sensitive elements (Ni, Mo, V, U) was performed by partial digestion using microwave digestion (Mars6; CEM Corporation). Sediment aliquots of 0.25 g we put into a PTFE vessel (EasyPrep) and was added 6 mL of HNO3 65% and 1 mL of HCl 27%. Both acids were previously purified by sub-boiling distillation using a quartz sub-boiling distillation system duo PUR (Milestone). Ten minutes after adding the acids, digestions were run in closed vessels for 30 minutes at 210 °C. Certified reference material as TILL-1 (CCRMP), BCR-2 and BHVO-2 (USGS) were also prepared to verify the accuracy of measurements.

With digestion complete, vessels were allowed to cool to room temperature before opening them. Samples were filtered and diluted to 50 mL with deionized water. For analysis in an ICP-MS iCAP Qc (Thermo Fisher Scientific), the working standard solutions were prepared by diluting the stock solutions 1000 mg L^{-1} in 2% nitric acid to obtain a concentration ranges of calibration solutions for all elements from 0.10 to 100 µg L^{-1}. Rhodium (Rh) 10 µg L^{-1} was used as internal standard to check the drift during analysis, and measurements were performed in KED mode. All analyses were performed at itt OCEANEON (UNISINOS University).

4. RESULTS

4.1 Correlation with previous studies

Our section is located in the same area as in the works of Guex et al. (2012), Schaltegger et al. (2008), Schoene et al. (2010), Wotzlaw et al. (2014) and Yager et al. (2017), spanning the Raethian-Hettangian interval. Our TOC series enables a direct correlation with the TOC data of Yager et al. (2017) (Fig. 2) and, consequently, the succession described by Schaltegger et al. (2008). Therefore, during the fieldwork, we located in our section stratigraphic positions of U-Pb dating published by Guex et al., 2012 and Wotzlaw et al., 2014) as well as the position of ammonite events according to Yager et al. (2017). The last occurrence of *Choristoceras crickmayi* marks the onset of the late Triassic extinction (ETE; just before 201.51 ± 0.15 Ma; Wotzlaw et al., 2014), whereas the first occurrence of *Psiloceras spelae* characterizes the TJB (TJB; 201.36 ± 0.17 Ma; Wotzlaw et al., 2014). We could not represent all ash layers in the studies section because of limitations of the graphic scale, since they range from millimeter to centimeter in thickness, and several ash levels can be found within a single meter. Thus we focus on the ash layers dated by

Guex et al. (2012), Schaltegger et al. (2008), Schoene et al. (2010) and Wotzlaw et al. (2014) which characterize the T-J transition. Later, we used these dated ash layers to derive an age model for the studied section Supplementary Table S3.

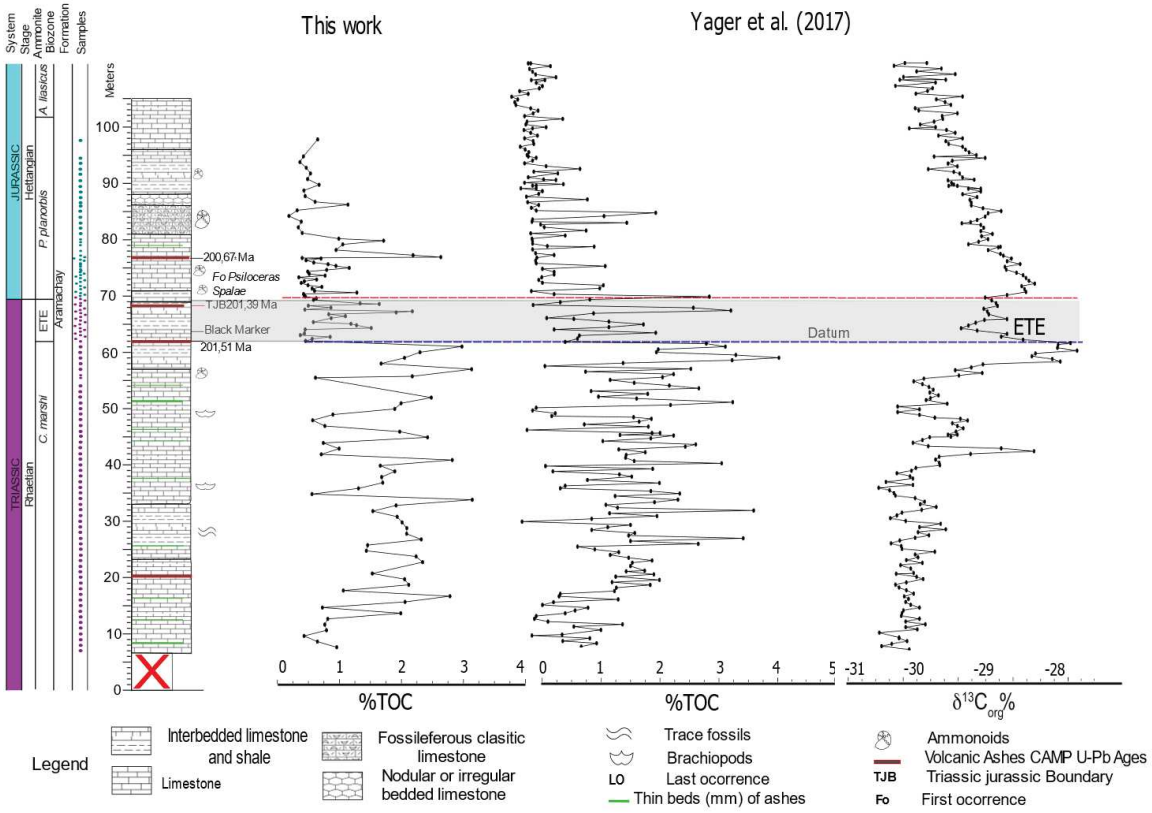

Fig. 2 - Correlation between our TOC record and the TOC and cacarbon isotope () records of Yager et al. (2017) for the same section. The red dashed line marks the TJB, and the blue dashed line marks chosen correlation datum (marked TOC drop). The end Triassic extinction (ETE) is marked as a light gray shading.

4.2 Proxies for weathering intensity, and carbonate and organic carbon preservation

Within the Raethian, log(K/Fe) shows a negative excursion in the basal portion of the ~14 m section (Fig. 3). It is followed by an interval characterized by low

amplitude oscillations, with a progressive overall K enrichment between ~10 and ~60 m. Near the onset of the end Triassic extinction (ETE) interval, just below the TJB, a marked negative excursion, from -0.83 to -1.02 log(K/Fe), occurs. Log(K/Fe) recovers to pre-excursion values at ~77 m in the section, ~7 m above the TJB (Fig. 3).

Within the Raethian interval, average $CaCO_3$ is 46.7% and average TOC is 1.8% (Fig. 3). Slightly below the ETE, there are increases of both TOC and $CaCO_3$, reaching maxima of 3.6% and 76%, respectively. At the TJB, TOC values drop from 1.2 to 0.7% and remain relatively low up to the top of the section, except by a positive excursion centered at ~77 m. As a result, $CaCO_3$ content falls at the TJB by about 70%, showing high-amplitude variability up to ~75 m in the section (Fig. 3). At ~77 m, the CaCO3 content recovers the pre-excursion values, but presenting high-amplitude oscillations.

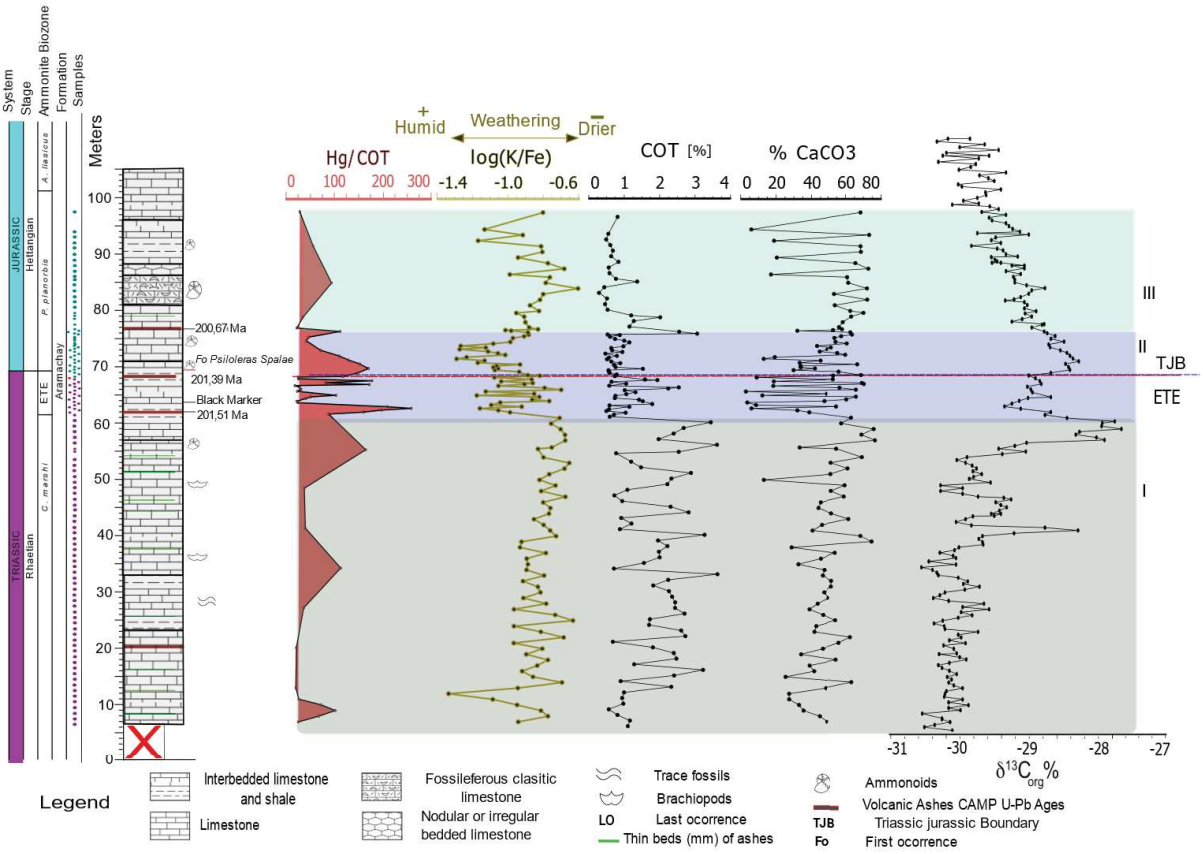

Fig. 3 - Paleoclimatic, paleoceanografic and volcanic activity proxies at the Levanto-Maino Section. We present Hg/TOC log(K/Fe), $CaCO_3$ content (%), and TOC content (%). The $\delta^{13}C_{org}$ data series is from Yager et al. (2017); the dashed red line marks the TJB, and intervals I to III characterize different hydrolimate settings.

4.3 Proxies for volcanic activity

The Levanto-Maino Section records three peaks of mercury (Hg) enrichment, even when normalized against TOC content. The first Hg enrichment peak occurs at the extinction horizon (62 m), the second and highest peak occurs at ~70 m (TJB), and the last and smaller peak occurs within the Hettangian (Fig. 3). Mercury concentrations and the Hg/TOC ratio present mean values of 51.5 µg/kg and 60.3, respectively, for the Raethian interval in the Levanto-Maino section (Fig. 3; only

Hg/TOC are shown). Both proxies peaked above 204 µg/kg (Hg concentration) and 259.6 (Hg/TOC ratio) at the center of the ETE interval (~65 m). After the ETE within the Hettangian interval, there are two smaller (than in the extinction horizon), followed by a gradual decline for both proxies within the Hettangian (Fig. 3).

4.4 Proxies for bottom water redox condition during the ETE

During the ETE, the redox ratios Mo/U, V(V+Ni), Ni/Co, and V/Cr present mean values of 3.37, 0.63, 6.8, 2.47, respectively (Fig. 4).

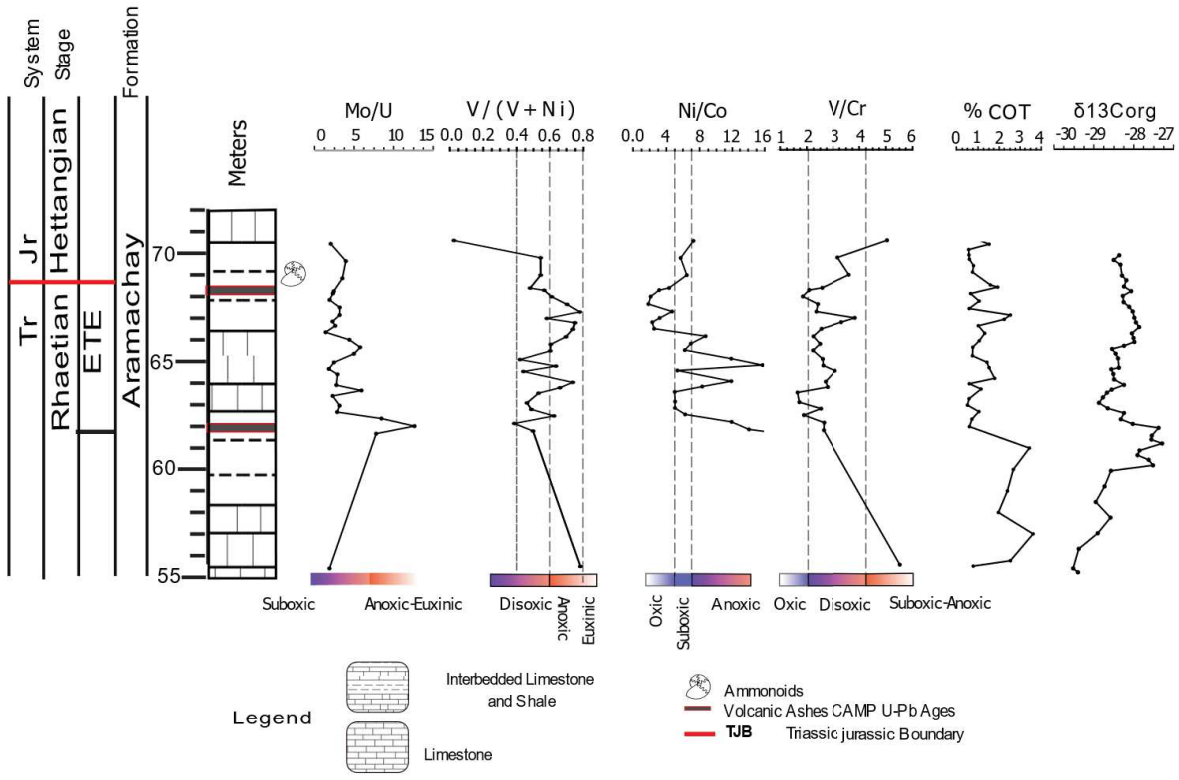

Fig. 4 Detailed view of the TJB at the Levanto-Maino section with paleoredox proxies. The $\delta^{13}C_{org}$ data series is from Yager et al. (2017).

5 DISCUSSIONS

5.1 *Hydroclimate changes across the TJB*

The Mesozoic was generally a warmer period than the present day, about 6 °C or more (Sellwood and Valdes, 2006). This was due to the configuration of the continents that were united in a single land mass forming a supercontinent (Pangea), which was centered on the at the Equator and emerged and was spreading between 85° N and 90° S (Ziegler et al., 1982). Modeling studies of Late Triassic evaporation and precipitation indicate a hot semi-arid to arid climate (Simms and Ruffell, 1989; Whiteside et al., 2011). These relatively arid global climate conditions remained until the end of the Triassic, when a mass extinction occurred associated with drastic climate changes (Preto et al., 2010). This climate change would be driven by the emission of volcanic greenhouse gases by the CAMP (Hesselbo et al., 2002; McElwain et al., 1999).

Our log(K/Fe) records at the Levanto-Maino section depict remarkable regional climate reorganizations during the TJB interval. Potassium is mainly delivered to deep ocean sediments in the structure of phyllosilicates such as illite (Yarincik et al., 2000), which is usually formed in relatively dry regions with low chemical weathering rates (Zabel et al., 2001). Iron is a main component of siliciclastic deep ocean sediments (Arz et al., 1998; Kwiecien et al., 2009), being mainly delivered by suspended riverine input of oxi-hydroxides, generated under wet climate conditions (e.g., Arz et al., 1998; Govin et al., 2012; Mulitza et al., 2008). Thus, we interpret that the Levanto-Maino section recorded relatively drier climatic conditions during the Triassic (Raethian), evidenced by relatively high log(K/Fe) values (Fig. 3 and 5; interval I). This climatic state transitioned to a relatively wetter

configurations that began within the Late Triassic ETE interval, just before the TJB, as evidenced by a sharp drop of log(K/Fe) at 62 m in the Levanto-Maino section (Fig. 3 and 5; interval II), which is correlated with the onset of negative CIE (Yager et al., 2017). Drier climate conditions were recorded again above ~76 m at the Levanto-Maino section (Fig. 3 and 5; interval III).

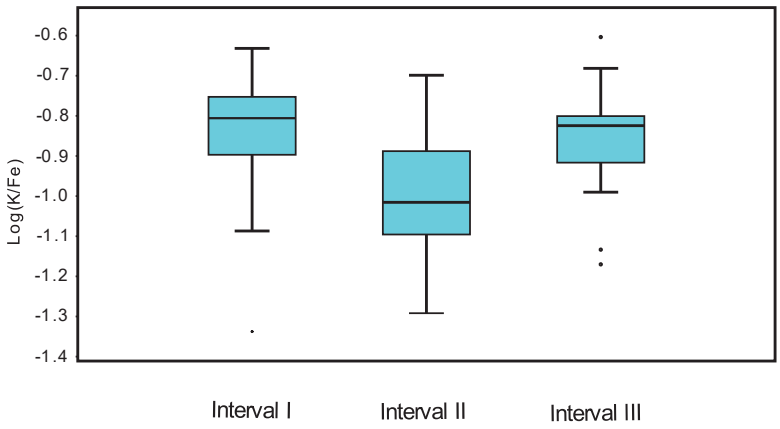

Fig. 5 Log 10 -scaled boxplots of the log (K/Fe) data in each age range (million years) of the Levanto-Maino section. Numbers of measurements samples (n): Interval I (202.6-201.5 Ma; n = 55), interval II (201.5-200.7 Ma; n = 46), interval III (200.7-199.0 Ma; n = 22). As identified in Fig. 3

This observation is in line with the onset of the environmental disturbances described (Hesselbo et al., 2002, 2007) at various locations in Europe for marine and non-marine settings (Guex et al., 2004; Hesselbo et al., 2002, 2007; Sellwood and Valdes, 2006; Williford et al., 2007). In southern Sweden, the Skåne the Kagerod Formation (upper Norian) is dominated by smectites, and transitions to kaolinite-rich clays in the Högana Formation (Raethian-Hettangian), which suggests a transition to warmer and wetter climate conditions (Ahlberg et al., 2003). This transition was also

observed in the Tratan Mountains, in the Furkaska section of Slovakia. In these sections smectite and illite-rich clays indicate an arid climate for the Fatra Formation (Rhaetian) and transition to kaolinite-enriched clays in the Kopeniac Formation (Hettangian), indicating the onset of greenhouse humid conditions (Michalík et al., 2010, 2013). A change in palynomorph assemblages at the TJB boundary was observed in the Furkaska section (Ruckwied and Götz, 2009), where a spore shift was associated with a sudden increase in humidity. According to Bonis et al. (2010) this shift to greenhouse conditions, with increased freshwater runoff, is also recorded by mineralogical and palynological data from the Kendlbach Formation in Austria. Mineralogical studies of late Triassic strata in Germany, with trilete spores (Van De Schootbrugge et al., 2009), suggest the onset of climate humid conditions. Our interpretations are consistent with Iqbal et al. (2019), who analyzed weathering trends in the Salt Range, Pakistan, using the chemical index of alteration (CIA) as well as clays and paleosol analyses. These authors suggests the occurrence of a relatively arid climate in the Triassic, evidenced by high illite contents, lower values of CIA and poorly drained paleosols, and wetter climate conditions at the TJB, as evidenced by increased abundance of kaolinite in paleosols and high CIA values in laterite/bauxite horizons.

The onset of this hydroclimate reorganization is marked by a negative CIE at the Levanto-Maino Section (Fig. 3) and at other TJB sections (Guex et al., 2004; Hesselbo et al., 2002; Williford et al., 2007). For instance in the northern calcareous Alps, Austria, a change in the weathering regime was also observed at the TJB, which is interpreted as a consequence of a transient shift to greenhouse climate conditions, and correlates with the onset of a major negative CIE (Pálfy and Zajzon, 2012). In the Levanto-Maino Section, the onset of the climatic reorganization

precisely coincides with the beginning of the CIE (Fig. 6), but peak wet climatic conditions occurred after the TJB, between 70 and 75 m in the section (Fig. 3). We suggest that increased weathering intensity at the TJB may have acted as a negative feedback mechanism that help withdrawing atmospheric CO_2 (e.g., Foster et al., 2018) released by CAMP activity (see Section 5.3).

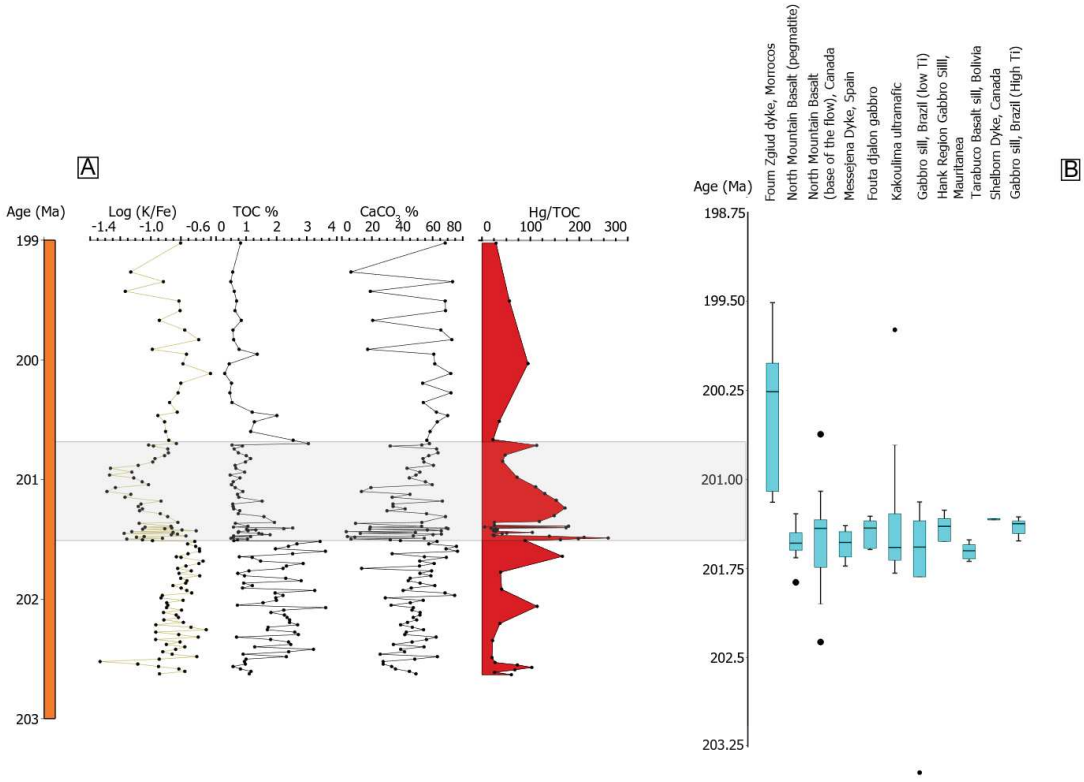

Figure 6 (A)- Paleoclimatic, paleoceanografic and volcanic activity proxies plotted against the age model for the Levanto-Maino Section based on dated vulcanic ash layers (Suplemmentary table s3) We present Hg/TOC log(K/Fe), $CaCO_3$ content (%), and TOC content (%). (B)- Log 10 -scaled boxplots of the age range (million years-Ma) in each incursion based in the dataset of Davies et. al (2017), and the age range obtained in this work. Numbers of measurements by incursions: Foum Zgiud dyke, Morocco = 7, North Mountain Basalt (pegmatite lens) = 10, North Mountain Basalt, base of the flow = 13, Messejana dyke = 8, Fouta Djalon gabbro sill = 7, Kakoulima, ultramafic Guinea = 16, gabbro sill= 9, Hank region gabbro sill = 7, Tarabuco basalt sill = 5, Shelborne dyke = 2, gabbro sill, Brazil = 9.

5.2 Carbon cycle perturbation and bottom water oxygenation at the TJB

Disruptions of the carbon cycle occurred during the Late Triassic and were recorded in several basins worldwide (Bachan et al., 2012; Fujisaki et al., 2016; Hesselbo et al., 2020, 2002; Lindström et al., 2017b), including the Levanto-Maino section (Yager et al. (2017). These disruptions were captured in the geological record as multiple positive and negative CIEs. The magnitudes and duration of the Levanto-Maino CIEs were discussed in Yager et al. (2017), dividing CIEs into three groups. First, there is a positive $\delta^{13}C_{org}$ excursion below the extinction horizon, followed by a negative excursion that starts at the extinction horizon, which is followed by a second positive excursion at the TJB, followed by the early Jurassic recovery to pre-disturbance levels.

In our work, TOC concentrations were high within the Raethian, peaked in tandem with the positive CIE preceding the TJB, and remained low throughout the Hettangian (Fig. 3). Therefore, we assume that organic carbon burial and/or preservation were enhanced before TJB and decreased afterward at the Levanto-Maino Section. Comparable trends were identified by Yager et al. (2017) at the Levanto-Maino section and mainly interpreted in terms of changing regimes of surface productivity. However, opposite trends were observed in European sections (Hesselbo et al., 2002), where bottom-water anoxia may have increased organic matter preservation during the Hettangian (Michalík et al., 2010; Van de Schootbrugge et al., 2013; Yager et al., 2017). Our proxy records suggest that

bottom waters remained oxic-dysoxic during the CIE that preceded the TJB at the Levanto-Maino Section (ETE interval; Fig. 4). Thus, we suggest that organic matter preservation is not the main factor controlling TOC content at the Levanto-Maino Section. Our findings, therefore, support the interpretation of Yager et al. (2017) that surface productivity changes controlled TOC content variability at the studied succession.

Based on model calculations, Huynh and Poulsen (2005) proposed that increased pCO_2 led to deep ocean oxygen depletion at the TJB. Some works, such as that of Bonis et al. (2010), suggest anoxia in tethyan sections. Based on biomarkers, euxinic conditions have been also proposed for shallow marine sediments deposited in the Tethys and Panthalasa oceans during the TJB (Richoz et al., 2012 Richoz et al., 2012 Jaraula et al., 2013 Kasprak et al., 2015). Our redox element data point to a different oxygenation setting at TJB boundary at the Levanto-Maino section, where the oxygenation conditions suggest the occurrence of general oxic to disoxic bottom water conditions and not anoxic conditions as suggested in other sections. This pattern could be related to paleogeographic conditions of Levanto-Maino Section. Fujisaki et al. (2018) analyzed the Katsuyama section (Japan) that records the TJB. They observed that the development of anoxia and euxinia was recorded only in shallow water environments, which would have probably been caused by intensification of continental weathering that would promote primary productivity and accumulation of organic matter.

Between 60 and 80 m at the Levanto-Maino Section, $CaCO_3$ content depicts high-amplitude oscillations (Fig. 3). Marked drops of $CaCO_3$ content occurred in tandem with the negative CIE recognized by Yager et al. (2017) at the Levanto-Maino Section at the TJB (Fig. 3). In many European basins, the negative CIE

interval is characterized by a collapse of carbonate productivity (Greene et al., 2012). Although a biotic crisis of calcifying organisms occurred at the time, when primary production may have shifted to a biogenic/non-skeletal mode (van de Schootbrugge et al., 2007). Other factors such as carbonate dissolution and dilution by terrigenous components may have played an important role in controlling carbonate accumulation (e.g., Zeebe and Zachos, 2007). In fact, Quan et al. (2008) suggested that increased input of terrigenous material drove the drop in carbonate content recorded at the Mingolsheim TJB Section in Germany. The increase in weathering rates across the TJB was detected by a sharp increase in a $^{187}Os/^{188}Os$ isotope record from England (Cohen and Coe, 2002). According to Fujisaki et al. (2018) this process resulted in increased continental runoff and, consequently, increased input of terrigenous components. The increase in continental runoff may also have promoted primary productivity in shallow environments, which could lead to the accumulation of organic matter in the bottom sediments and explain the occurrence of anoxic-euxinic conditions (Hallam, 1995). It is also likely that oscillations in carbonate content at the Levanto-Maino Section between 60 and 80 m were controlled by dilution by terrigenous components since this interval was also characterized by a shift to wet climate conditions (see section 5.1). We also assume that the deposition of volcanic ash could dilute the $CaCO_3$ content during the ETE, along the TJB, and between 85 and 97.5 m in the studied section (Fig. 3). However, we cannot rule out a possible carbonate dissolution effect, as calcareous fossils are relatively rare throughout the succession.

5.3 Volcanic trigger for environmental changes across the TJB

Our data demonstrate an enrichment in Hg and Hg/TOC values during ETE and at the TJB at the Levanto-Maino section (Fig. 3). Hg/TOC enrichments recorded in Phanerozoic sediments range between 400 and 800 ppb/wt. %. Mercury spikes correlate with three of the five major depletions of Fanerozoic biodiversity (see Charbonnier et al., 2020). Grasby et al. (2019) point to the difficulties in interpreting Hg/TOC peaks when TOC is <0.2% since it could induce to biases of Hg/TOC values. Fortunately, our values are within expectations when compared to the Hg/TOC of Percival et al. (2017) and Thibodeau et al. (2016), with the lowest TOC value of 0.27% (usually varying from 0.4 to 3.7%). These observations imply that the trends depicted at the Levanto-Maino section are indeed robust. Another aspect that could influence Hg deposition would be the presence of sulfides (Shen et al., 2020, 2019), still, neither petrographic slides (Yager et al., 2017) nor field evidence supports the presence of pyrite in the studied section. Shen et al. (2020) suggested that values of total sulfur (TS) >1.0% and TS/TOC >0.35 generally conform to a sulfide host phase for Hg, whereas TS <1.0% or TS/TOC <0.35 suggests an organic host phase. At the Levanto-Maino Section, mean TS is 0.16 and mean TS/TOC is 0.13, thus excluding a Hg enrichment controlled by S host phases (online supplementary material Table S4). According to Shen et al. (2020), high sedimentation rates could also influence Hg concentrations, since they tend to dilute the main sediment components (organic matter, sulfides) that store Hg. Additionally, peaks of Hg/TOC at the studied section occur in an interval characterized by relative wet climate conditions and increased continental runoff when sedimentation rates were likely to be relatively high. However, Mercury Independent Fractionation data from Yager et al. (2021) for the Levanto-Maino Section also suggest that the section

was not receiving Hg from continental runoff, once this type of Hg enrichment would be more common in shallow marine settings (Them et al., 2019).

Our peaks of Hg concentrations and the Hg/TOC ratio are correlated with a well-constrained negative CIE (Fig. 6) suggesting that this is not a local feature of the Lavanto-Maino Section, but instead the record of a global signal related to the TJB environmental perturbation. Several works in Triassic-Jurassic successions (Kovács et al., 2020; Percival et al., 2017; Ruhl et al., 2020; Thibodeau et al., 2016; Yager et al., 2021) demonstrate this relationship between negative CIEs and enrichment in Hg. For instance, Thibodeau et al. (2016), studying the TJB section of Muller Canyon, Nevada, found peaks of Hg and Hg/COT in the late Triassic correlated with a negative CIE with low TOC. Yager et al. (2021), comparing the TJB records of Hg/TOC of Levanto-Maino Section with the basins of St. Audrie's bay (England), Lombardia (Italy), Monte Sparagio (Sicily), and New York Canyons Nevada, identified the Hg/TOC remained high during the Hettangian. However, this pattern does not appear in our record, possibly due to the lower sampling resolution of our study. High Hg/TOC values after the TJB were also observed in other basins by Percival et al. (2017), who presented a correlation between six different locations in North and South America, Europe and Africa. These authors also noticed that five of the six analyzed sessions recorded Hg enrichments at the TJB, at the extinction level, and associated with carbon cycle disturbances.

Percival et al. (2017) correlated the oldest preserved fluxes of the CAMP with Hg enrichment levels in the sedimentary record. This correlation supports a volcanic origin for the increases in sedimentary Hg around the TJB. Davies et al. (2017) mapped and dated the CAMP intrusions that precede the TJB, which could have triggered environment instability, with the oldest CAMP intrusions dated as

201.635±0.029 Ma. Median ages of these intrusions are correlated with age estimated for the highest Hg enrichment peak at the Levanto-Maino section (~201.5 Ma; Fig. 6), making us suggest that the hydroclimate reorganization described here was, in fact, triggered by CAMP volcanic activity. However, Hg concentrations and Hg/TOC remained high until ~200.1 Ma at the Levanto-Maino section (Yager et al., 2021), suggesting that local depositional and/or diagenetic processes may have also influenced Hg concentration and the Hg/TOC ratio (Yager et al., 2021).

6 CONCLUSIONS

Here we analyzed the deep marine Levanto-Maino section, Peru, seeking to correlate geochemical proxies for climate and paleoceanographic conditions across the TJB with tracers for CAMP volcanic activity. Our main conclusion are:

- We note that the Levanto-Maino section records a hydroclimate shift from relatively dry conditions at the end of the Triassic to wetter climate conditions, associated with increased terrigenous input, at the Triassic-Jurassic transition. This interval of climate change is coeval with the beginning of CAMP volcanic activity.
- Volcanic activity is indirectly recorded at the studied section by peaks of Hg concentrations and the Hg/TOC ratio, which were coeval with the negative CIE associated with the first CAMP intrusions that preceded the TJB.
- Bottom water were oxic to dysoxic at TJB, suggesting that anoxia during the Triassic-Jurassic transition was mostly restricted to shallow marine settings.

Our results highlight the potential of the Levanto-Maino section in improving our understanding of ETE and TJB at deep marine settings, since we can correlate climatic and paleoceanographic reorganizations with trends identified worldwide.

ACKNOWLEDGEMENTS

The authors are grateful to the Nova Analítica company for kindly granting the Direct Mercury Analyzer (DMA-80 evo) for use in our laboratory. E. M. F. thanks the Coordination Foundation for the Improvement of Higher Education Personnel (CAPES) for the granted scholarship. We also thank the staff at itt OCEANEON, for assistance with analyses and discussions, especially Jorge. V. Martín for help with constructing box plots.

REFERÊNCIAS

Ahlberg, A., Olsson, I., Šimkevičius, P., 2003. Triassic-Jurassic weathering and clay mineral dispersal in basement areas and sedimentary basins of southern Sweden. Sediment. Geol. 161, 15–29. https://doi.org/10.1016/S0037-0738(02)00381-0

Alroy, J., 2010. Fair Sampling of Taxonomic Richness and Unbiased Estimation of Origination and Extinction Rates. Paleontol. Soc. Pap. 16, 55–80. https://doi.org/10.1017/s1089332600001819

Arz, H.W., Pätzold, J., Wefer, G., 1998. Correlated millennial-scale changes in surface hydrography and terrigenous sediment yield inferred from Last-Glacial marine

deposits off northeastern Brazil. Quat. Res. 50, 157–166. https://doi.org/10.1006/qres.1998.1992

Bachan, A., Payne, J.L., 2016. Modelling the impact of pulsed CAMP volcanism on pCO2 and δ13C across the Triassic-Jurassic transition. Geol. Mag. 153, 252–270. https://doi.org/10.1017/S0016756815000126

Bachan, A., Van De Schootbrugge, B., Fiebig, J., McRoberts, C.A., Ciarapica, G., Payne, J.L., 2012. Carbon cycle dynamics following the end-Triassic mass extinction: Constraints from paired δ13Ccarb and δ13Corg records. Geochemistry, Geophys. Geosystems 13, 1–24. https://doi.org/10.1029/2012GC004150

Blackburn, T.J., Olsen, P.E., Bowring, S.A., McLean, N.M., Kent, D. V., Puffer, J., McHone, G., Rasbury, E.T., Et-Touhami, M., 2013. Zircon U-Pb geochronology links the end-triassic extinction with the central Atlantic magmatic province. Science (80-.). 340, 941–945. https://doi.org/10.1126/science.1234204

Bonis, N.R., Ruhl, M., Kürschner, W.M., 2010. Climate change driven black shale deposition during the end-Triassic in the western Tethys. Palaeogeogr. Palaeoclimatol. Palaeoecol. 290, 151–159. https://doi.org/10.1016/j.palaeo.2009.06.016

Charbonnier, G., Adatte, T., Föllmi, K.B., Suan, G., 2020. Effect of Intense Weathering and Postdepositional Degradation of Organic Matter on Hg/TOC Proxy in Organic-rich Sediments and its Implicationsfor Deep-Time Investigations. Geochemistry, Geophys. Geosystems 21. https://doi.org/10.1029/2019GC008707

Cohen, A.S., Coe, A., 2002. New geochemical evidence for the onset of volcanism in the Central Atlantic magmatic province and environmental change at the Triassic-Jurassic boundary. Geology 30, 267–270.

https://doi.org/https://doi.org/10.1130/0091-7613(2002)030<0267:NGEFTO>2.0.CO;2

Croudace, I.W., Rothwell, R.G., 2015. Micro-XRF Studies of Sediment Cores: Aplications of a non-destrutive tool for the environmental sciences, 17th ed. Canada.

Foster, G.L., Hull, P., Lunt, D.J., Zachos, J.C., 2018. Placing our current “hyperthermal” in the context of rapid climate change in our geological past. Philos. Trans. R. Soc. A Math. Phys. Eng. Sci. https://doi.org/10.1098/rsta.2017.0086

Fujisaki, W., Matsui, Y., Asanuma, H., Sawaki, Y., Suzuki, K., Maruyama, S., 2018. Global perturbations of carbon cycle during the Triassic–Jurassic transition recorded in the mid-Panthalassa. Earth Planet. Sci. Lett. 500, 105–116. https://doi.org/10.1016/j.epsl.2018.07.026

Fujisaki, W., Sawaki, Y., Yamamoto, S., Sato, T., Nishizawa, M., Windley, B.F., Maruyama, S., 2016. Tracking the redox history and nitrogen cycle in the pelagic Panthalassic deep ocean in the Middle Triassic to Early Jurassic: Insights from redox-sensitive elements and nitrogen isotopes. Palaeogeogr. Palaeoclimatol. Palaeoecol. 449, 397–420. https://doi.org/10.1016/j.palaeo.2016.01.039

Govin, A., Holzwarth, U., Heslop, D., Ford Keeling, L., Zabel, M., Mulitza, S., Collins, J.A., Chiessi, C.M., 2012. Distribution of major elements in Atlantic surface sediments (36°N-49°S): Imprint of terrigenous input and continental weathering. Geochemistry, Geophys. Geosystems 13, 1–23. https://doi.org/10.1029/2011GC003785

Grasby, S.E., Them, T.R., Chen, Z., Yin, R., Ardakani, O.H., 2019. Mercury as a proxy for volcanic emissions in the geologic record. Earth-Science Rev. 196, 102880. https://doi.org/10.1016/j.earscirev.2019.102880

Greene, S.E., Martindale, R.C., Ritterbush, K.A., Bottjer, D.J., Corsetti, F.A., Berelson, W.M., 2012. Recognising ocean acidification in deep time: An evaluation of the evidence for acidification across the Triassic-Jurassic boundary. Earth-Science Rev. 113, 72–93. https://doi.org/10.1016/j.earscirev.2012.03.009

Guex, J., Bartolini, A., Atudorei, V., Taylor, D., 2004. High-resolution ammonite and carbon isotope stratigraphy across the Triassic-Jurassic boundary at New York Canyon (Nevada). Earth Planet. Sci. Lett. 225, 29–41. https://doi.org/10.1016/j.epsl.2004.06.006

Guex, J., Schoene, B., Bartolini, A., Spangenberg, J., Schaltegger, U., O'Dogherty, L., Taylor, D., Bucher, H., Atudorei, V., 2012. Geochronological constraints on post-extinction recovery of the ammonoids and carbon cycle perturbations during the Early Jurassic. Palaeogeogr. Palaeoclimatol. Palaeoecol. 346–347, 1–11. https://doi.org/10.1016/j.palaeo.2012.04.030

Hallam, A., 1995. Oxygen-restricted facies of the basal jurassic of north west europe. Hist. Biol. 10, 247–257. https://doi.org/10.1080/10292389509380523

Hallam, A., Wignall, P.B., 1999. Mass extinctions and sea-level changes. Earth Sci. Rev. 48, 217–250. https://doi.org/10.1016/S0012-8252(99)00055-0

Hautmann, M., Benton, M.J., Tomašových, A., 2008. Catastrophic ocean acidification at the Triassic-Jurassic boundary. Neues Jahrb. fur Geol. und Palaontologie - Abhandlungen 249, 119–127. https://doi.org/10.1127/0077-7749/2008/0249-0119

Hesselbo, S.P., Korte, C., Ullmann, C. V., Ebbesen, A.L., 2020. Carbon and oxygen isotope records from the southern Eurasian Seaway following the Triassic-Jurassic boundary: Parallel long-term enhanced carbon burial and seawater warming. Earth-Science Rev. 203, 103131. https://doi.org/10.1016/j.earscirev.2020.103131

Hesselbo, S.P., McRoberts, C.A., Pálfy, J., 2007. Triassic-Jurassic boundary events: Problems, progress, possibilities. Palaeogeogr. Palaeoclimatol. Palaeoecol. 244, 1–10. https://doi.org/10.1016/j.palaeo.2006.06.020

Hesselbo, S.P., Robinson, S.A., Surlyk, F., Piasecki, S., 2002. Terrestrial and marine extinction at the Triassic-Jurassic boundary synchronized with major carbon-cycle perturbation: A link to initiation of massive volcanism? Geology 30, 251–254. https://doi.org/10.1130/0091-7613(2002)030<0251:TAMEAT>2.0.CO;2

Hillebrandt, A. v., 1994. The Triassic/Jurassic boundary and Hettangian biostratigraphy in the area of the Utcubamba valley (Northern Peru). Geobios 27, 297–307. https://doi.org/10.1016/S0016-6995(94)80148-7

Hillebrandt, A. V., Krystyn, L., Kürschner, W.M., Bonis, N.R., Ruhl, M., Richoz, S., Schobben, M.A., Urlichs, M., Bown, P.R., Kment, K., McRoberts, C.A., Simms, M., Tomãsových, A., 2013. The global stratotype sections and point (GSSP) for the base of the jurassic system at kuhjoch (Karwendel Mountains, Northern Calcareous Alps, Tyrol, Austria). Episodes 36, 162–198. https://doi.org/10.18814/epiiugs/2013/v36i3/001

Huynh, T.T., Poulsen, C.J., 2005. Rising atmospheric CO2 as a possible trigger for the end-Triassic mass extinction. Palaeogeogr. Palaeoclimatol. Palaeoecol. 217, 223–242. https://doi.org/10.1016/j.palaeo.2004.12.004

Iqbal, S., Wagreich, M., Irfan U, J., Kuerschner, W.M., Gier, S., Bibi, M., 2019. Hot-house climate during the Triassic/Jurassic transition: The evidence of climate change from the southern hemisphere (Salt Range, Pakistan). Glob. Planet. Change 172, 15–32. https://doi.org/10.1016/j.gloplacha.2018.09.008

Jaeschke, A., Rühlemann, C., Arz, H., Heil, G., Lohmann, G., 2007. Coupling of millennial-scale changes in sea surface temperature and precipitation off

northeastern Brazil with high-latitude climate shifts during the last glacial period. Paleoceanography 22, 1–10. https://doi.org/10.1029/2006PA001391

Jaraula, C.M.B., Grice, K., Twitchett, R.J., Böttcher, M.E., LeMetayer, P., Dastidar, A.G., Opazo, L.F., 2013. Elevated pCO2 leading to late triassic extinction, persistent photic zone euxinia, and rising sea levels. Geology 41, 955–958. https://doi.org/10.1130/G34183.1

Kasprak, A.H., Sepúlveda, J., Price-Waldman, R., Williford, K.H., Schoepfer, S.D., Haggart, J.W., Ward, P.D., Summons, R.E., Whiteside, J.H., 2015. Episodic photic zone euxinia in the northeastern Panthalassic Ocean during the end-Triassic extinction. Geology 43, 307–310. https://doi.org/10.1130/G36371.1

Kovács, E.B., Ruhl, M., Demény, A., Fórizs, I., Hegyi, I., Horváth-Kostka, Z.R., Móricz, F., Vallner, Z., Pálfy, J., 2020. Mercury anomalies and carbon isotope excursions in the western Tethyan Csővár section support the link between CAMP volcanism and the end-Triassic extinction. Glob. Planet. Change 194, 103291. https://doi.org/10.1016/j.gloplacha.2020.103291

Kwiecien, O., Arz, H.W., Lamy, F., Plessen, B., Bahr, A., Haug, G.H., 2009. North Atlantic control on precipitation pattern in the eastern Mediterranean/Black Sea region during the last glacial. Quat. Res. 71, 375–384. https://doi.org/10.1016/j.yqres.2008.12.004

Lindström, S., van de Schootbrugge, B., Hansen, K.H., Pedersen, G.K., Alsen, P., Thibault, N., Dybkjær, K., Bjerrum, C.J., Nielsen, L.H., 2017a. A new correlation of Triassic–Jurassic boundary successions in NW Europe, Nevada and Peru, and the Central Atlantic Magmatic Province: A time-line for the end-Triassic mass extinction. Palaeogeogr. Palaeoclimatol. Palaeoecol. 478, 80–102. https://doi.org/10.1016/j.palaeo.2016.12.025

Lindström, S., van de Schootbrugge, B., Hansen, K.H., Pedersen, G.K., Alsen, P., Thibault, N., Dybkjær, K., Bjerrum, C.J., Nielsen, L.H., 2017b. A new correlation of Triassic–Jurassic boundary successions in NW Europe, Nevada and Peru, and the Central Atlantic Magmatic Province: A time-line for the end-Triassic mass extinction. Palaeogeogr. Palaeoclimatol. Palaeoecol. 478, 80–102. https://doi.org/10.1016/j.palaeo.2016.12.025

Marzoli, A., Bertrand, H., Knight, K.B., Cirilli, S., Buratti, N., Vérati, C., Nomade, S., Renne, P.R., Youbi, N., Martini, R., Allenbach, K., Neuwerth, R., Rapaille, C., Zaninetti, L., Bellieni, G., 2004. Synchrony of the Central Atlantic magmatic province and the Triassic-Jurassic boundary climatic and biotic crisis. Geology 32, 973–976. https://doi.org/10.1130/G20652.1

Marzoli, A., Davies, J.H.F.L., Youbi, N., Merle, R., Dal Corso, J., Dunkley, D.J., Fioretti, A.M., Bellieni, G., Medina, F., Wotzlaw, J.F., McHone, G., Font, E., Bensalah, M.K., 2017. Proterozoic to Mesozoic evolution of North-West Africa and Peri-Gondwana microplates: Detrital zircon ages from Morocco and Canada. Lithos 278–281, 229–239. https://doi.org/10.1016/j.lithos.2017.01.016

Marzoli, A., Melluso, L., Morra, V., Renne, P.R., Sgrosso, I., D'Antonio, M., Duarte Morais, L., Morais, E.A.A., Ricci, G., 1999. Geochronology and petrology of Cretaceous basaltic magmatism in the Kwanza basin (western Angola), and relationships with the Parana-Etendeka continental flood basalt province. J. Geodyn. 28, 341–356. https://doi.org/10.1016/S0264-3707(99)00014-9

McElwain, J.C., Beerling, D.J., Woodward, F.I., 1999. Fossil plants and global warming at the Triassic-Jurassic boundary. Science (80-.). 285, 1386–1390. https://doi.org/10.1126/science.285.5432.1386

Michalík, J., Biroň, A., Lintnerová, O., Götz, A.E., Ruckwied, K., 2010. Climate change

at the triassic/jurassic boundary in the northwestern tethyan realm, inferred from sections in the tatra Mountains (Slovakia). Acta Geol. Pol. 60, 535–548.

Michalík, J., Lintnerová, O., Wójcik-Tabol, P., Gaådzicki, A., Grabowski, J., Golej, M., Šimo, V., Zahradníková, B., 2013. Paleoenvironments during the Rhaetian transgression and the colonization history of marine biota in the Fatric Unit (Western Carpathians). Geol. Carpathica 64, 39–62. https://doi.org/10.2478/geoca-2013-0003

Mulitza, S., Prange, M., Stuut, J.B., Zabel, M., Von Dobeneck, T., Itambi, A.C., Nizou, J., Schulz, M., Wefer, G., 2008. Sahel megadroughts triggered by glacial slowdowns of Atlantic meridional overturning. Paleoceanography 23, 1–11. https://doi.org/10.1029/2008PA001637

Olsen, P.E., 2002. Ascent of Dinosaurs Linked to an Iridium Anomaly at the Triassic-Jurassic Boundary. Science (80-.). 296, 1305–1307. https://doi.org/10.1126/science.1065522

Pálfy, J., Demény, A., Hass, J., Hetényi, M., Orchard, M.J., Vetö, I., 2001. Carbon isotope anomaly and other geochemical changes at the Triassic-Jurassic boundary from a marine section in Hungary. Geology 29, 1047–1050. https://doi.org/10.1130/0091-7613(2001)029<1047:CIAAOG>2.0.CO;2

Pálfy, J., Zajzon, N., 2012. Environmental changes across the Triassic-Jurassic boundary and coeval volcanism inferred from elemental geochemistry and mineralogy in the Kendlbachgraben section (Northern Calcareous Alps, Austria). Earth Planet. Sci. Lett. 335–336, 121–134. https://doi.org/10.1016/j.epsl.2012.01.039

Paris, G., Beaumont, V., Bartolini, A., Clémence, M.E., Gardin, S., Page, K., 2010. Nitrogen isotope record of a perturbed paleoecosystem in the aftermath of the

end-Triassic crisis, Doniford section, SW England. Geochemistry, Geophys. Geosystems 11, 1–15. https://doi.org/10.1029/2010GC003161

Percival, L.M.E., Ruhl, M., Hesselbo, S.P., Jenkyns, H.C., Mather, T.A., Whiteside, J.H., 2017. Mercury evidence for pulsed volcanism during the end-Triassic mass extinction. Proc. Natl. Acad. Sci. U. S. A. 114, 7929–7934. https://doi.org/10.1073/pnas.1705378114

Preto, N., Kustatscher, E., Wignall, P.B., 2010. Triassic climates - State of the art and perspectives. Palaeogeogr. Palaeoclimatol. Palaeoecol. 290, 1–10. https://doi.org/10.1016/j.palaeo.2010.03.015

Quan, T.M., van de Schootbrugge, B., Field, M.P., Rosenthal, Y., Falkowski, P.G., 2008. Nitrogen isotope and trace metal analyses from the Mingolsheim core (Germany): Evidence for redox variations across the Triassic-Jurassic boundary. Global Biogeochem. Cycles 22, 1–14. https://doi.org/10.1029/2007GB002981

Raup, D.M., Sepkoski, J.J., 1982. Mass Extinctions in the Marine Fossil Record. Am. Assoc. Adv. Sci. Stable 4539, 215.

Richoz, S., Van De Schootbrugge, B., Pross, J., Püttmann, W., Quan, T.M., Lindström, S., Heunisch, C., Fiebig, J., Maquil, R., Schouten, S., Hauzenberger, C.A., Wignall, P.B., 2012. Hydrogen sulphide poisoning of shallow seas following the end-Triassic extinction. Nat. Geosci. 5, 662–667. https://doi.org/10.1038/ngeo1539

Rosas, S., Fontboté, L., Tankard, A., 2007. Tectonic evolution and paleogeography of the Mesozoic Pucará Basin, central Peru. J. South Am. Earth Sci. 24, 1–24. https://doi.org/10.1016/j.jsames.2007.03.002

Ruckwied, K., Götz, A., 2009. Climate change at the Triassic/Jurassic boundary: Palynological evidence from the Furkaska section (Tatra Mountains, Slovakia).

Geol. Carpathica 60, 139–149. https://doi.org/10.2478/v10096-009-0009-0

Ruhl, M., Bonis, N.R., Reichart, G.J., Sinninghe Damsté, J.S., Kürschner, W.M., 2011. Atmospheric carbon injection linked to end-Triassic mass extinction. Science (80-.). 333, 430–434. https://doi.org/10.1126/science.1204255

Ruhl, M., Hesselbo, S.P., Al-Suwaidi, A., Jenkyns, H.C., Damborenea, S.E., Manceñido, M.O., Storm, M., Mather, T.A., Riccardi, A.C., 2020. On the onset of Central Atlantic Magmatic Province (CAMP) volcanism and environmental and carbon-cycle change at the Triassic–Jurassic transition (Neuquén Basin, Argentina). Earth-Science Rev. 208, 103229. https://doi.org/10.1016/j.earscirev.2020.103229

Schaller, M.F., Wright, J.D., Kent, D. V., Olsen, P.E., 2012. Rapid emplacement of the Central Atlantic Magmatic Province as a net sink for CO 2. Earth Planet. Sci. Lett. 323–324, 27–39. https://doi.org/10.1016/j.epsl.2011.12.028

Schaltegger, U., Guex, J., Bartolini, A., Schoene, B., Ovtcharova, M., 2008. Precise U-Pb age constraints for end-Triassic mass extinction, its correlation to volcanism and Hettangian post-extinction recovery. Earth Planet. Sci. Lett. 267, 266–275. https://doi.org/10.1016/j.epsl.2007.11.031

Schoene, B., Guex, J., Bartolini, A., Schaltegger, U., Blackburn, T.J., 2010. Correlating the end-Triassic mass extinction and flood basalt volcanism at the 100 ka level. Geology 38, 387–390. https://doi.org/10.1130/G30683.1

Sellwood, B.W., Valdes, P.J., 2006. climas Mesozóico : modelos gerais de circulação e o disco de rock 190, 269–287.

Sepkoski, J.J., 1996. Patterns of Phanerozoic Extinction: a Perspective from Global Data Bases. Glob. Events Event Stratigr. Phaneroz. 35–51. https://doi.org/10.1007/978-3-642-79634-0_4

Shen, J., Algeo, T.J., Chen, J., Planavsky, N.J., Feng, Q., Yu, J., Liu, J., 2019. Mercury in marine Ordovician/Silurian boundary sections of South China is sulfide-hosted and non-volcanic in origin. Earth Planet. Sci. Lett. 511, 130–140. https://doi.org/10.1016/j.epsl.2019.01.028

Shen, J., Feng, Q., Algeo, T.J., Liu, Jinling, Zhou, C., Wei, W., Liu, Jiangsi, Them, T.R., Gill, B.C., Chen, J., 2020. Sedimentary host phases of mercury (Hg) and implications for use of Hg as a volcanic proxy. Earth Planet. Sci. Lett. 543, 1–13. https://doi.org/10.1016/j.epsl.2020.116333

Simms, M.J., Ruffell, A.H., 1989. Synchroneity of climatic change and extinctions in the Late Triassic. Geology 17, 265–268. https://doi.org/10.1130/0091-7613(1989)017<0265:SOCCAE>2.3.CO;2

Tankard, 2002. Tectonic Framework of Basin Evolution in Peru by Tankard Enterprises Ltd . for. Petroperu S.a.

Them, T.R., Jagoe, C.H., Caruthers, A.H., Gill, B.C., Grasby, S.E., Gröcke, D.R., Yin, R., Owens, J.D., 2019. Terrestrial sources as the primary delivery mechanism of mercury to the oceans across the Toarcian Oceanic Anoxic Event (Early Jurassic). Earth Planet. Sci. Lett. 507, 62–72. https://doi.org/10.1016/j.epsl.2018.11.029

Thibodeau, A.M., Ritterbush, K., Yager, J.A., West, A.J., Ibarra, Y., Bottjer, D.J., Berelson, W.M., Bergquist, B.A., Corsetti, F.A., 2016. Mercury anomalies and the timing of biotic recovery following the end-Triassic mass extinction. Nat. Commun. 7. https://doi.org/10.1038/ncomms11147

Tjallingii, R., Stattegger, K., Wetzel, A., Van Phach, P., 2010. Infilling and flooding of the Mekong River incised valley during deglacial sea-level rise. Quat. Sci. Rev. 29, 1432–1444. https://doi.org/10.1016/j.quascirev.2010.02.022

Van de Schootbrugge, B., Bachan, A., Suan, G., Richoz, S., Payne, J.L., 2013.

Microbes, mud and methane: Cause and consequence of recurrent early Jurassic anoxia following the end-Triassic mass extinction. Palaeontology 56, 685–709. https://doi.org/10.1111/pala.12034

Van De Schootbrugge, B., Payne, J.L., Tomasovych, A., Pross, J., Fiebig, J., Benbrahim, M., Föllmi, K.B., Quan, T.M., 2008. Carbon cycle perturbation and stabilization in the wake of the Triassic-Jurassic boundary mass-extinction event. Geochemistry, Geophys. Geosystems 9. https://doi.org/10.1029/2007GC001914

Van De Schootbrugge, B., Quan, T.M., Lindström, S., Püttmann, W., Heunisch, C., Pross, J., Fiebig, J., Petschick, R., Röhling, H.G., Richoz, S., Rosenthal, Y., Falkowski, P.G., 2009. Floral changes across the Triassic/Jurassic boundary linked to flood basalt volcanism. Nat. Geosci. 2, 589–594. https://doi.org/10.1038/ngeo577

van de Schootbrugge, B., Tremolada, F., Rosenthal, Y., Bailey, T.R., Feist-Burkhardt, S., Brinkhuis, H., Pross, J., Kent, D. V., Falkowski, P.G., 2007. End-Triassic calcification crisis and blooms of organic-walled “disaster species.” Palaeogeogr. Palaeoclimatol. Palaeoecol. 244, 126–141. https://doi.org/10.1016/j.palaeo.2006.06.026

Von Hillebrandt, A., 2000. The ammonoid fauna of the south American Hettangian (basal Jurassic): Part III. Palaeontogr. Abteilung A Palaozoologie - Stratigr. 258, 65–116.

Ward, P.D., Haggart, J.W., Carter, E.S., Wilbur, D., Tipper, H.W., Evans, T., 2001. Sudden productivity collapse associated with the Triassic-Jurassic boundary mass extinction. Science (80-.). 292, 1148–1151. https://doi.org/10.1126/science.1058574

Weltje, G.J., Tjallingii, R., 2008. Calibration of XRF core scanners for quantitative

geochemical logging of sediment cores: Theory and application. Earth Planet. Sci. Lett. 274, 423–438. https://doi.org/10.1016/j.epsl.2008.07.054

Whiteside, J.H., Grogan, D.S., Olsen, P.E., Kent, D. V., 2011. Climatically driven biogeographic provinces of Late Triassic tropical Pangea. Proc. Natl. Acad. Sci. U. S. A. 108, 8972–8977. https://doi.org/10.1073/pnas.1102473108

Whiteside, J.H., Olsen, P.E., Kent, D. V., Fowell, S.J., Et-Touhami, M., 2007. Synchrony between the Central Atlantic magmatic province and the Triassic-Jurassic mass-extinction event? Palaeogeogr. Palaeoclimatol. Palaeoecol. 244, 345–367. https://doi.org/10.1016/j.palaeo.2006.06.035

Williford, K.H., Ward, P.D., Garrison, G.H., Buick, R., 2007. An extended organic carbon-isotope record across the Triassic-Jurassic boundary in the Queen Charlotte Islands, British Columbia, Canada. Palaeogeogr. Palaeoclimatol. Palaeoecol. 244, 290–296. https://doi.org/10.1016/j.palaeo.2006.06.032

Wotzlaw, J.F., Guex, J., Bartolini, A., Gallet, Y., Krystyn, L., McRoberts, C.A., Taylor, D., Schoene, B., Schaltegger, U., 2014. Towards accurate numerical calibration of the late triassic: Highprecision U-Pb geochronology constraints on the duration of the Rhaetian. Geology 42, 571–574. https://doi.org/10.1130/G35612.1

Yager, J.A., West, A.J., Corsetti, F.A., Berelson, W.M., Rollins, N.E., Rosas, S., Bottjer, D.J., 2017. Duration of and decoupling between carbon isotope excursions during the end-Triassic mass extinction and Central Atlantic Magmatic Province emplacement. Earth Planet. Sci. Lett. 473, 227–236. https://doi.org/10.1016/j.epsl.2017.05.031

Yager, J.A., West, A.J., Thibodeau, A.M., Corsetti, F.A., Rigo, M., Berelson, W.M., Bottjer, D.J., Greene, S.E., Ibarra, Y., Jadoul, F., Ritterbush, K.A., Rollins, N., Rosas, S., Di Stefano, P., Sulca, D., Todaro, S., Wynn, P., Zimmermann, L.,

Bergquist, B.A., 2021. Mercury contents and isotope ratios from diverse depositional environments across the Triassic–Jurassic Boundary: Towards a more robust mercury proxy for large igneous province magmatism. Earth-Science Rev. 223, 103775. https://doi.org/10.1016/j.earscirev.2021.103775

Yarincik, K.M., Murray, R.W., Peterson, L.C., 2000. Climatically sensitive eolian and hemipelagic deposition in the Cariaco Basin, Venezuela, over the past 578,000 years: Results from Al/Ti and K/Al. Paleoceanography 15, 210–228. https://doi.org/10.1029/1999PA900048

Zabel, M., Schneider, R.R., Wagner, T., Adegbie, A.T., De Vries, U., Kolonic, S., 2001. Late quaternary climate changes in central Africa as inferred from terrigenous input to the Niger fan. Quat. Res. 56, 207–217. https://doi.org/10.1006/qres.2001.2261

Zeebe, R.E., Zachos, J.C., 2007. Reversed deep-sea carbonate ion basin gradient during Paleocene-Eocene thermal maximum. Paleoceanography 22, 1–17. https://doi.org/10.1029/2006PA001395

Ziegler, A.M., Scotese, C.R., Barrett, S.F., 1982. Mesozoic and Cenozoic paleogeographic maps. Tidal Frict. Earth's Rotat. II. Proc. Work. Bielefeld, 1981 240–252. https://doi.org/10.1007/978-3-642-68836-2_17